

## Article

# Marine-Inspired Ovoidiol Analogs Inhibit Membrane-Bound Gamma-Glutamyl-Transpeptidase and Modulate Reactive Oxygen Species and Glutathione Levels in Human Leukemic Cells

Annalisa Zuccarotto <sup>1</sup>, Maria Russo <sup>2</sup>, Annamaria Di Giacomo <sup>2</sup>, Alessandra Casale <sup>1</sup>, Aleksandra Mitrić <sup>3</sup>, Serena Leone <sup>4</sup>, Gian Luigi Russo <sup>2</sup> and Immacolata Castellano <sup>1,4,\*</sup>

- <sup>1</sup> Department of Molecular Medicine and Medical Biotechnology, University of Naples Federico II, 80131 Naples, Italy; annalisa.zuccarotto@unina.it (A.Z.); ales.casale@studenti.unina.it (A.C.)  
<sup>2</sup> National Research Council, Institute of Food Sciences, 83100 Avellino, Italy; maria.russo@isa.cnr.it (M.R.); annamariadigiacomio90@gmail.com (A.D.G.); gianluigi.russo@cnr.it (G.L.R.)  
<sup>3</sup> Institute of Clinical and Molecular Virology, Friedrich-Alexander University Erlangen-Nürnberg, 91054 Erlangen, Germany; aleksandra.mitric27@gmail.com  
<sup>4</sup> Department of Biology and Evolution of Marine Organisms, Stazione Zoologica Anton Dohrn, Villa Comunale, 80121 Naples, Italy; serena.leone@szn.it  
\* Correspondence: immacolata.castellano@unina.it

## Abstract

The enzyme  $\gamma$ -glutamyl transpeptidase (GGT), located on the surface of cellular membranes, hydrolyzes extracellular glutathione (GSH) to guarantee the recycling of cysteine and maintain intracellular redox homeostasis. High expression levels of GGT on tumor cells are associated with increased cell proliferation and resistance against chemotherapy. Therefore, GGT inhibitors have potential as adjuvants in treating GGT-positive tumors; however, most have been abandoned during clinical trials due to toxicity. Recent studies indicate marine-derived ovoidiols as more potent non-competitive GGT inhibitors, inducing a mixed cell-death phenotype of apoptosis and autophagy in GGT-overexpressing cell lines, such as the chronic B leukemic cell HG-3, while displaying no toxicity towards non-proliferative cells. In this work, we characterize the activity of two synthetic ovoidiol analogs, L-5-sulfanylhistidine and iso-ovoidiol A, in GGT-positive cells, such as HG-3 and HL-60 cells derived from acute promyelocytic leukemia. The two compounds inhibit the activity of membrane-bound GGT, without altering cell vitality nor inducing cytotoxic autophagy in HG-3 cells. We provide evidence that a portion of L-5-sulfanylhistidine enters HG-3 cells and acts as a redox regulator, contributing to the increase in intracellular GSH. On the other hand, ovoidiol A, which is mostly sequestered by external membrane-bound GGT, induces intracellular ROS increase and the consequent autophagic pathways. These findings provide the basis for developing ovoidiol derivatives as adjuvants in treating GGT-positive tumors' chemoresistance.

**Keywords:** ovoidiols; 5-thiohistidine; gamma-glutamyl-transpeptidase; glutathione; GGT inhibitors; leukemic cells



Academic Editor: Sergey A. Dyshlovoy

Received: 3 June 2025

Revised: 18 July 2025

Accepted: 25 July 2025

Published: 30 July 2025

**Citation:** Zuccarotto, A.; Russo, M.; Di Giacomo, A.; Casale, A.; Mitrić, A.; Leone, S.; Russo, G.L.; Castellano, I. Marine-Inspired Ovoidiol Analogs Inhibit Membrane-Bound Gamma-Glutamyl-Transpeptidase and Modulate Reactive Oxygen Species and Glutathione Levels in Human Leukemic Cells. *Mar. Drugs* **2025**, *23*, 308. <https://doi.org/10.3390/md23080308>

**Copyright:** © 2025 by the authors. Licensee MDPI, Basel, Switzerland. This article is an open access article distributed under the terms and conditions of the Creative Commons Attribution (CC BY) license (<https://creativecommons.org/licenses/by/4.0/>).

## 1. Introduction

Glutamyl transpeptidase (GGT) is an enzyme localized on the cellular membrane, where it catalyzes the hydrolysis of extracellular glutathione (GSH,  $\gamma$ -L-glutamyl-L-cysteinylglycine) [1]. It is synthesized as a unique polypeptide, which undergoes an

autocleavage into a large and a small subunit, interacting to form a functional dimer with the active site directed towards the extracellular space [2]. Human GGTs are glycoproteins, and their molecular mass varies, due to the different degrees of protein glycosylation [3,4]. The physiological substrate GSH is biosynthesized in the cytosol and is considered the most abundant antioxidant thiol in the cell [5]. Under oxidative stress conditions, GSH can be oxidized to its disulfide GSSG, and the excess of both forms can be effluxed into the extracellular environment through multidrug-resistance-associated proteins [6,7]. There, membrane-bound GGT cleaves the peculiar  $\gamma$ -glutamyl bond between glutamate and the amino group of cysteine in GSH [8,9]. Then, membrane-bound dipeptidases hydrolyze the resulting cysteinyl-glycine to release glycine and cysteine, which are finally transported into the cell by neutral amino acid transporters [10]. In the cell, these amino acids serve as a source for the de novo synthesis of GSH and proteins [11]. Therefore, in humans, where GSH acts as a key antioxidant molecule, GGT plays a pivotal role in GSH metabolism and in balancing cellular redox homeostasis [12–14]. Previous work reported that GGT-deficient mice display delayed growth, associated with significantly higher GSH concentrations in plasma (175  $\mu$ M) and urine (15.4  $\mu$ M) compared to wild-type mice (27.6  $\mu$ M and 6.2  $\mu$ M, respectively), and ultimately die due to cysteine deficiency [15]. These mice are more susceptible to oxidative stress and lung injury than wild-type mice [16]. Several human tumors, including hepatocellular carcinoma and renal cell carcinoma, exhibit high levels of GGT activity, which enhances their ability to recycle GSH [17–20]. Consequent elevated intracellular GSH levels contribute to chemo- and radiotherapy resistance and prevent the initiation of the apoptotic cascade in tumor cells [20]. When inhibiting GGT activity for 2 h, the intracellular cysteine concentration in GGT-positive tumors was significantly reduced [21,22]. In leukemia cells, the drug-resistant lines displayed 3-fold higher GGT activity and intracellular GSH levels, allowing cells to metabolize more extracellular GSH and take up more cysteine [23]. Several studies have suggested that the same mechanism could confer GGT-positive tumors resistance to pro-oxidant anticancer therapies, including platinum-based compounds, alkylating agents, and radiation [19,23]. Therefore, intense efforts have been continuously devoted to identifying new GGT inhibitors to potentially ameliorate the treatment of pathologies associated with high levels of GGT activity, such as cancer, ischemia–reperfusion-induced renal injury, asthma, and liver fibrosis [24].

The first compounds to show GGT-inhibitory activity included glutamine analogs and other aminoacidic derivatives such as acivicin, 6-diazo-5-oxo-L-norleucine, azaserine [25,26], sulfur derivatives of L-glutamic acid, and  $\gamma$ -(monophenyl) phosphonoglutamate analogs [27]. However, most of these compounds have displayed toxicity due to their interference with essential metabolic pathways [24–26]. Among monophenyl phosphonoglutamate analogs, only the butanoic acid derivative GGT<sub>Top</sub> has been reported to be less toxic [27] and effective for treating asthma and oral mucositis [28,29]. Another class of less toxic and uncompetitive inhibitors has been developed from benzene-sulfonamide (OU749) [30]. Recently, OU749 has been encapsulated in a supramolecular platinum prodrug nano-assembly delivery system for the chemotherapy of cisplatin-resistant cancer [31]. This strategy has been shown to efficiently reduce GGT activity and intracellular GSH levels, thereby augmenting peroxides and preventing chemoresistance. We have recently focused on a class of 5-(N)-methyl thiohistidines, sulfur-containing natural products, known as ovothiols [32,33], which play a key role in controlling the cellular redox balance thanks to their ability to perform redox exchange with GSH [24,32]. Natural ovothiol A (ovo), isolated and characterized from the eggs of the sea urchin *Paracentrotus lividus* and abundant in other marine invertebrates [34], has been reported to inhibit membrane-bound GGT when administered in its disulfide form, and concomitantly induce autophagy in a human liver carcinoma cell line HepG2 and chronic B leukemic cells HG-3 [35–37]. Moreover, ovo has

been reported to exhibit GGT-inhibitory activity and an anti-inflammatory action on the livers of mice affected by liver fibrosis [38]. Overall, these studies have prompted the chemical synthesis and testing of marine-inspired ovo analogs [39].

Here, we report the biological effect of two synthetic ovo-related compounds—2-amino-3-(5-sulfanylimidazol-4-yl) propanoic acid, here referred to as L-5-sulfanyl histidine (5-thio), and 2-amino-3-(1-methyl-5-sulfanylimidazol-4-yl) propanoic acid, here referred to as iso-ovothiol A (iso-ovoA)—on GGT activity and GSH metabolism in human leukemic cells. Our results suggest that these compounds could be potentially employed as adjuvants for treating GGT-positive tumors and other diseases associated with elevated GGT activation.

## 2. Results

### 2.1. Marine-Inspired Ovothiol Analogs Inhibit Membrane-Bound GGT in GGT-Positive Cell Lines

HepG2 and HG-3 cells were previously tested for GGT expression and activity and recognized as a rich source of GGT [36]. Partially purified GGT extracts from HepG2 and HG-3, containing the mature membrane-bound form of GGT, were tested for residual GGT activity in the presence of 5-thio and iso-ovoA at different concentrations. The first compound, 5-thio, represents the unmethylated precursor of natural ovo. The second, iso-ovoA, differs from the natural compound due to the methylation site on the imidazole ring of histidine (Figure 1A). The two synthetic compounds were used in the disulfide form to avoid side reactions, as their thiol group displays a low pKa, associated with extreme reactivity [32]. Under these conditions, 50% GGT inhibition in HepG2 extracts was obtained at ~36  $\mu\text{M}$  for 5-thio and at ~59  $\mu\text{M}$  for iso-ovoA. Similarly, in HG-3 extracts, 50% GGT inhibition was obtained at ~32  $\mu\text{M}$  for 5-thio and at ~54  $\mu\text{M}$  for iso-ovoA. These results indicate that 5-thio induces significant inhibition of GGT, and is comparatively more efficient than iso-ovoA. Moreover, HepG2 extracts appeared slightly more resistant to GGT inhibition, likely due to the high grade of protein glycosylation [36]. Therefore, we continued evaluating GGT's residual activity on HG-3 cells, using 5-thio as the stronger ovothiol analog inhibitor. To confirm that 5-thio inhibits membrane-bound GGT in dividing cells, HG-3 cells were treated with 30  $\mu\text{M}$  of 5-thio, and residual GGT activity was measured after 30 min, 2 h, and 24 h. GGT-membrane-bound activity was significantly reduced after 30 min and 2 h of treatment in the presence of 5-thio (Figure 1B). On the contrary, we did not observe a significant reduction in GGT activity at 24 h. The inhibition of the membrane-bound GGT activity was confirmed by the increase in GSH levels in the extracellular medium at different incubation times, measured via an HPLC analysis (Figure 1C).

### 2.2. Ovothiol Analogs Are Not Cytotoxic in Human Leukemia Cells

To investigate the effects of marine-inspired ovo derivatives on cell proliferation, HG-3 and HL-60 cells of acute promyelocytic leukemia, both known for their GGT expression [36,40], were exposed to 5-thio and iso-ovoA at various concentrations for 24 h, and the results were compared with those of natural marine ovo. Treatment of HG3 with 5-thio showed no decrease in cell viability from 15  $\mu\text{M}$  to 100  $\mu\text{M}$ , with a slight increase noted at 15  $\mu\text{M}$  (Figure 2A). Similarly, treatment of HG-3 cells with iso-ovoA at concentrations up to 100  $\mu\text{M}$  did not lead to a significant decrease in cell viability, as measured by the CyQuant assay for proliferating cells (Figure 2B). In contrast, natural ovo caused a significant reduction in HG3 cell viability at a concentration of 20  $\mu\text{M}$  (Figure 2A). Similarly, the treatment with 5-thio and iso-ovoA did not significantly alter the cell viability of HL-60 cells (Figure 2C). On the contrary, natural ovo induced a significant reduction in HL-60 cell viability at 40  $\mu\text{M}$  (Figure 2C).

### 2.3. 5-Thio Does Not Modify Autophagy Flux in GGT-Positive HG-3 Cell Line

We previously demonstrated that natural ovo induces cytotoxic autophagy in HepG2 and HG-3 cells [35,36]. Here, we investigated whether a similar effect could be observed with the chemical derivative 5-thio, which inhibits human GGT with a slightly lower but significant strength. We quantified autophagic vacuoles using a Cyto-ID autophagy kit, which incorporates a green dye that fluoresces when taken up by pre-autophagosomes, autophagosomes, and autolysosomes. The green fluorescence, normalized to the total number of cells stained with Hoechst nuclear dye, revealed an increased presence of autophagic vacuoles in cells treated with ovo at 20  $\mu\text{M}$  compared to untreated control cells (Figure 3A,B), indicating altered autophagic flux. In contrast, treatment with 5-thio at 30  $\mu\text{M}$  did not lead to significant changes relative to untreated cells. As a positive control, HG-3 cells were treated with 40  $\mu\text{M}$  of chloroquine for 24 h (Figure 3A,B), which by blocking autophagy flux caused an accumulation of cytoplasmic autophagosomes. Under these conditions, fluorescence microscopy and image capture (micrographs in Figure 3A) confirmed the activation of cytotoxic autophagy by ovo in HG-3 cells.

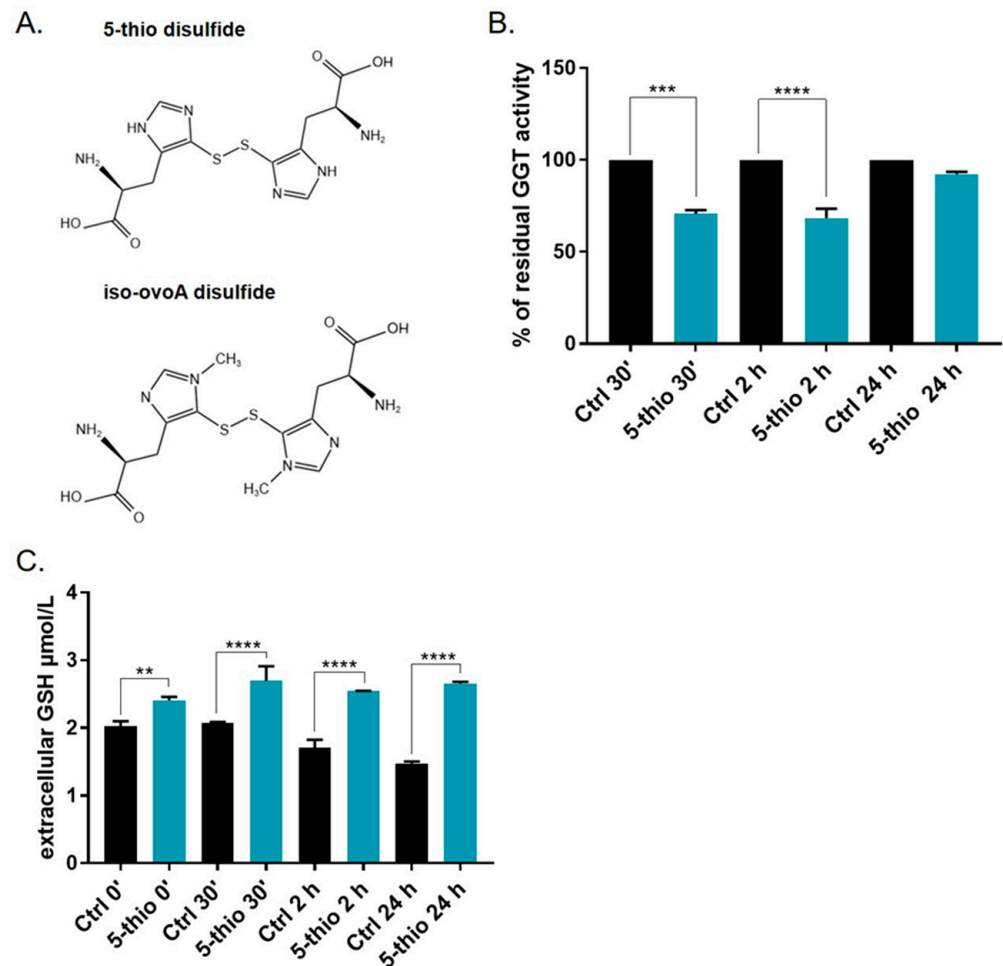


**Figure 1.** Disulfide structures of 5-thio and iso-ovoA (A). Membrane-bound GGT activity determination at different times after 30  $\mu\text{M}$  5-thio treatment in HG-3 (B). The percentages of GGT residual activity were compared to 100% activity of not-treated cells (Ctrl). Extracellular GSH determination via HPLC (C). The amounts of GSH at different times of 30  $\mu\text{M}$  5-thio treatment in HG-3 cells were compared to that in non-treated cells. A one-way ANOVA was used with a Tukey post hoc statistical analysis. Symbols indicate significance: \*\*  $p < 0.01$ ; \*\*\*  $p < 0.001$ ; \*\*\*\*  $p < 0.0001$ .

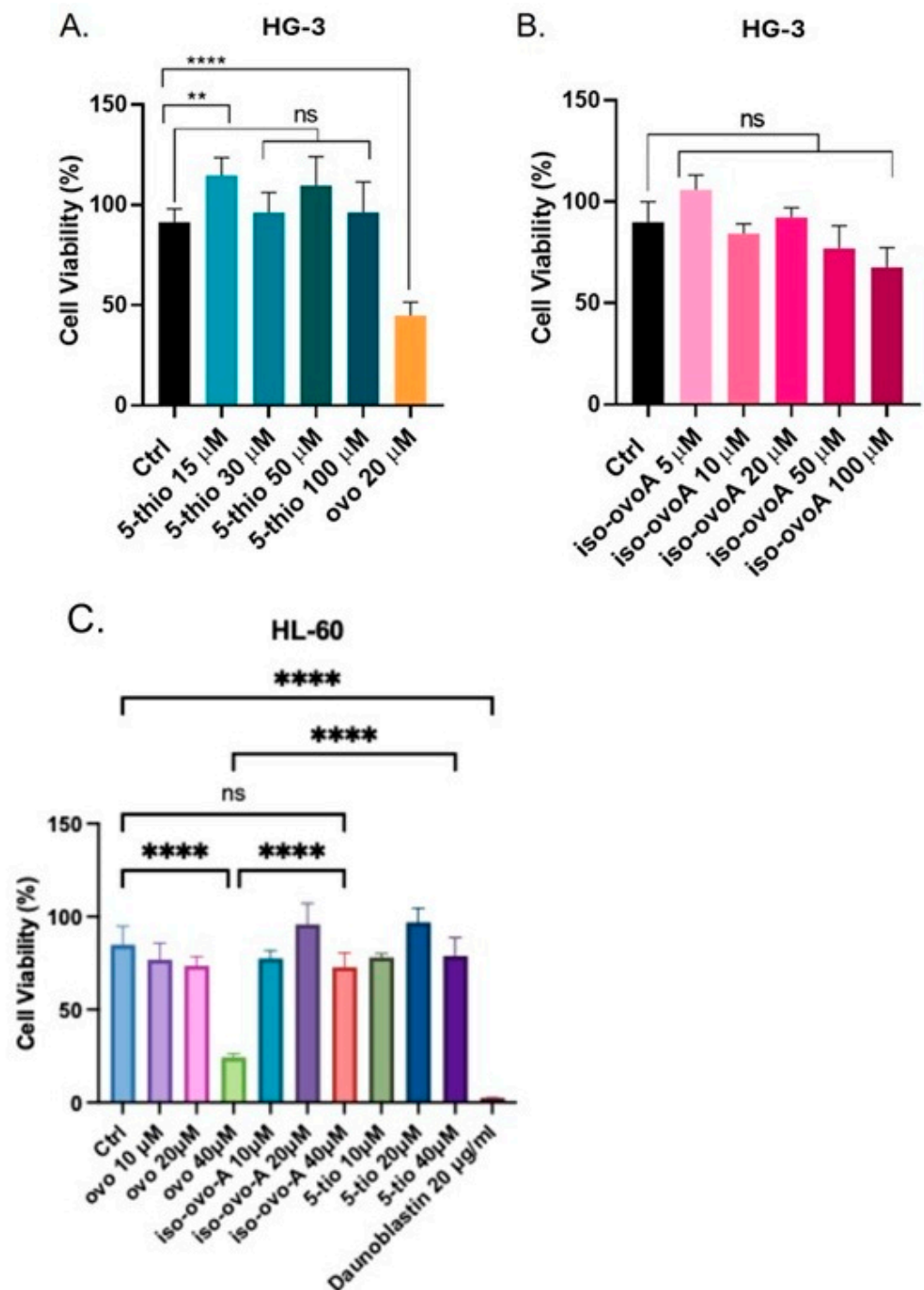


**Figure 2.** The HG-3 cells were treated with specified concentrations of the indicated compounds for 24 h at 37 °C in a 5% CO<sub>2</sub> incubator using a complete RPMI medium. The Cy-Quant cell viability assay was employed to evaluate the cytotoxicity of the reported concentrations of natural ovo and its analogs, 5-thio (A) and iso-ovoA (B). HL-60 cells were incubated with the indicated compounds, and a cell viability assay (Cy-Quant) was performed after 24 h (C). Daunoblastin, a cytotoxic drug, was used as a positive control. The fluorescence from viable cells (excitation at 485 nm/emission at 530 nm) was expressed as a percentage of untreated (Ctrl) cells. The bars in the graphs represent the mean of two independent experiments, each performed in quadruplicate. A one-way ANOVA was used with a Tukey post hoc statistical analysis. Symbols indicate significance: \*\*  $p < 0.01$ ; \*\*\*  $p < 0.0001$ ; ns: not significant.

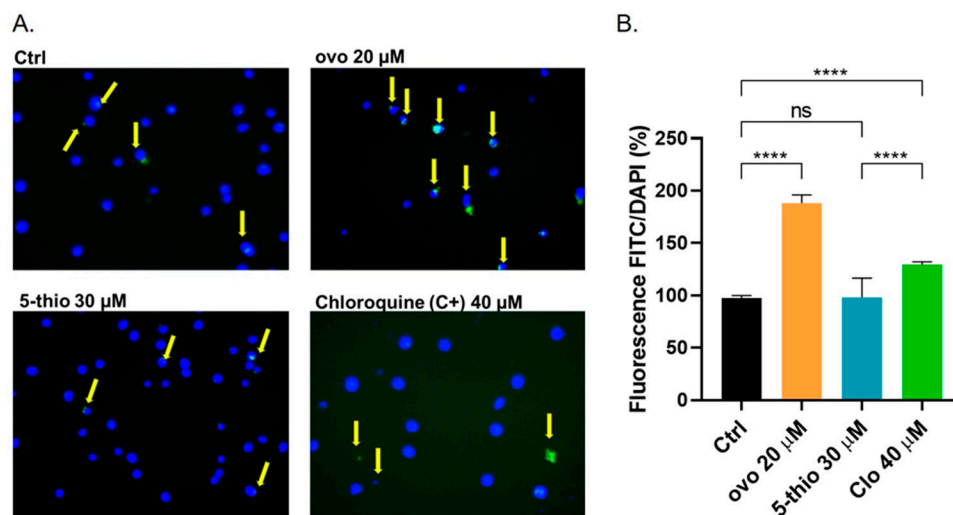


**Figure 3.** The HG-3 cells were treated with indicated concentrations of different compounds for 24 h at 37 °C with 5% CO<sub>2</sub> in a complete RPMI medium. Cyto-ID dye and Hoechst nuclear staining were added to the cells and incubated for 30 min. Cytoplasmic autophagosomes were monitored with an inverted microscope, and representative images were taken as reported in (A). Specific autophagosome staining (yellow arrows indicate the FITC-positive cells), calculated as fluorescence from the FITC/DAPI ratio, is expressed as a percentage of untreated (Ctrl) cells (B). Chloroquine (40 μM) was used as a positive control. In (B), bars indicate the mean of two experiments in quadruplicate. A one-way ANOVA was used with a Tukey post hoc statistical analysis. Symbols indicate significance: \*\*\*\*  $p < 0.0001$ ; ns: not significant.

#### 2.4. Bioavailability of 5-Thio in GGT-Positive HG-3 Cell Line

To assess the bioavailability of 5-thio in GGT-positive cell lines, we detected the extracellular and intracellular levels of 5-thio upon treatment of HG-3 cells at different times via HPLC, after derivatization of the samples with 4-bromomethyl-7-methoxycoumarin (BMC). We observed a significant time-dependent decrease in the extracellular levels of 5-thio at 30 min up to 24 h (Figure 4A). However, our data indicated that most of the administered 5-thio remained outside the cells, compatible with its interaction with GGT. On the other hand, we detected a significant peak of 5-thio in the intracellular extract of HG-3 cells treated with 5-thio soon after treatment, from 30 min to 24 h (Figure 4B). On the contrary, we did not observe any peak corresponding to natural ovo inside the cells after treatment of GGT-positive cell lines such as HepG2 [35].

#### 2.5. 5-Thio Modulates Intracellular ROS and GSH Levels in GGT-Positive HG-3 Cell Line

To investigate whether 5-thio, when administered in its disulfide form, can undergo redox exchange with GSH in the reducing intracellular environment, we assessed the levels of intracellular ROS using the CM-DCF-DA probe. As shown in Figure 5A, treatment with 30 μM of 5-thio resulted in a slight but not significant alteration of intracellular ROS levels after 30 min (>5%), while 20 μM ovo induced a higher increase (>10%) at the same time point. However, after 1 h of treatment with 30 μM of 5-thio, intracellular peroxide levels remained unchanged (Figure 5A). In contrast, treatment with 20 μM of natural ovo led to a significant increase in intracellular ROS after 1 h (>50%). On the other hand, the levels of intracellular GSH, detected via HPLC, significantly increased at 24 h of treatment with 5-thio compared to untreated cells (Figure 5B), likely suggesting an initial redox exchange of 5-thio with intracellular GSH, followed by an increase in GSH biosynthesis.

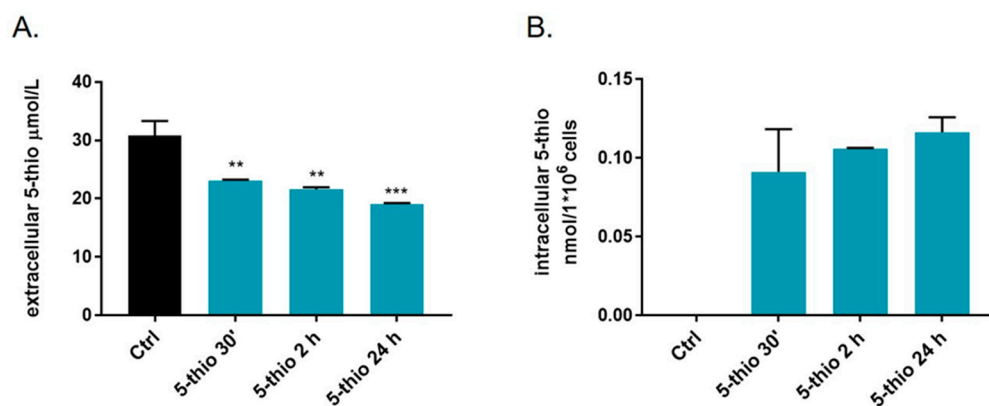


**Figure 4.** Determination of 5-thio bioavailability in the cell medium of HG-3 cell lines following drug treatment (A). Ctrl represents positive control, i.e., culture medium added with 30  $\mu\text{M}$  5-thio. Intracellular levels of 5-thio detected via HPLC at different times of 30  $\mu\text{M}$  5-thio treatment in HG-3 (B). Ctrl represents negative control (not treated cells, which have not incorporated 5-thio). A one-way ANOVA was used with a Tukey post hoc statistical analysis. Symbols indicate significance: \*\*  $p < 0.01$ ; \*\*\*  $p < 0.001$ .

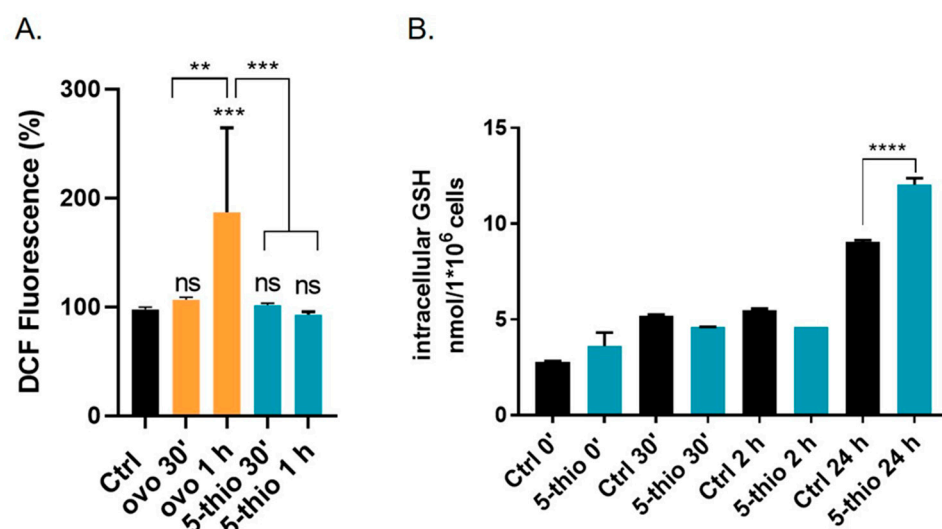


**Figure 5.** (A) Intracellular peroxide levels measured with fluorescent probe DCF in HG-3 cells treated for 30 min or 1 h with natural ovo or 5-thio at the indicated concentration. Peroxide levels were expressed as a percentage of DCF fluorescence (excitation at 485 nm/emission at 530 nm) compared to untreated cells (Ctrl). Data represent the mean of two experiments in quadruplicate. (B) Determination of intracellular GSH levels in HG-3 cell lines after 30  $\mu\text{M}$  5-thio treatment, compared to untreated cells (Ctrl). A one-way ANOVA was used with a Tukey post hoc statistical analysis. Symbols indicate significance: \*\*  $p < 0.01$ ; \*\*\*  $p < 0.001$ , \*\*\*\*  $p < 0.0001$ ; ns: not significant.

### 3. Discussion

Due to its involvement in GSH metabolism, drug detoxification, and the maintenance of cellular redox homeostasis, GGT plays a key role in the progression of different types of cancer [24,38]. In particular, in human tumors, where GGT is overexpressed, it induces new protein synthesis, cell proliferation, and resistance to chemo- and radiotherapy [23,41–44]. Therefore, some therapeutic strategies involve using GGT inhibitors to sensitize GGT-overexpressing tumors to chemotherapy [19,23]. For example, the administration of the GGT inhibitor acivicin in combination with chemotherapy in mice resulted in reduced intracellular GSH levels and the regression of metastatic melanoma in most of the animals tested [22,42]. Unfortunately, most GGT inhibitors developed to date, including acivicin, are too toxic for humans or do not display the efficacy desired for clinical use [24,25]. Therefore,

recent research has been devoted to discovering novel potent and nontoxic GGT inhibitors. Recently, we have demonstrated that the marine natural ovo strongly inhibits GGT activity and induces a mix of apoptosis and autophagy in GGT-overexpressing cell lines, including HepG2 and HG-3 [35,36]. However, the purification of such a compound from natural sources, such as sea urchins, requires many efforts and a large number of eggs [35]. This does not represent an ecologically sustainable task, also considering that sea urchins are a protected species. Therefore, in this work, we have investigated the GGT-inhibitory potential of two ovo analogs obtained via biomimetic chemical synthesis [39]. We previously confirmed that HepG2 and HG-3 cells overexpress GGT compared to nonmalignant tissue [36], making them a suitable target for testing potential GGT inhibitors. Using GGT activity assays, we observed that both compounds can inhibit GGT extracted from both HepG2 and HG-3 cells. In particular, 5-thio achieves a 50% reduction in enzymatic activity at a concentration of  $\sim 30 \mu\text{M}$  in HG-3 cells, which are more sensitive to GGT inhibition compared to HepG2, likely due to the lowest degree of GGT glycosylation. On the other hand, iso-ovo A is less potent than 5-thio, and both compounds display lower potency compared to natural ovo ( $K_i = 21 \mu\text{M}$ ) [36]. Our findings appear particularly surprising if we compare the results of cytotoxicity assays. Indeed, 5-thio and iso-ovo A did not display any significant effect on the cell vitality of leukemic cells, such as HG-3 and HL-60, both overexpressing GGT [36,40]. On the other hand, natural ovo caused significantly reduced cell vitality at  $20 \mu\text{M}$  in HG-3 and  $40 \mu\text{M}$  in HL-60 cells, confirming the ability to induce cell death through an autophagic pathway [36].

By inhibiting GGT activity and the extracellular GSH hydrolysis, we expect to find an increase in the extracellular pool of GSH and a decrease in the intracellular GSH levels [22,42]. This is the case for natural ovo, which was previously observed to inhibit membrane-bound GGT in HepG2 and HG-3 and induce the accumulation of extracellular GSH [36]. Therefore, to verify the occurrence of a similar behavior for the chemical derivative 5-thio, we employed thiol derivatization coupled with an HPLC analysis to measure the levels of GSH inside and outside HG-3 cells upon treatment with 5-thio. Indeed, we observed the accumulation of extracellular GSH in the medium, following 5-thio-induced inhibition of membrane-bound GGT activity (Figure 1). Furthermore, we observed the uptake of intracellular 5-thio with its concomitant decrease in the extracellular medium (Figure 4). This indicates that part of the free 5-thio, not involved in the interaction with membrane-bound GGT, entered the cells, where the intracellular pool of GSH is expected to reduce it [39,45]. Once reduced, intracellular 5-thio may act as an antioxidant and contribute to the fight against the increased pool of ROS in cells (Figure 6). This is likely why we observed only a slightly but not significant increased level of intracellular ROS after 30 min of 5-thio treatment, followed by a balance of intracellular ROS at 1 h of treatment. On the contrary, ovo supplementation increased intracellular ROS levels at 30 min and more significantly after 1 h of treatment (Figure 5A). Indeed, since ovo is a more potent inhibitor of GGT compared to 5-thio, the effects of its action on the decrease in intracellular GSH levels should be more evident compared to 5-thio. In our previous work, we did not detect ovo inside GGT-positive cells such as HepG2, thereby suggesting that most ovo in its disulfide form interacts with membrane-bound GGT and the free form does not enter the cells at appreciable levels [35]. This may explain why, in the case of ovo, the effect on the inhibition of GGT and the blockage of GSH recycling overcomes the potential of the thiol to act as an intracellular antioxidant. Indeed, in the case of ovo, we observed an increase in intracellular ROS, which likely contributes to the induction of a mixed phenotype of autophagy and apoptosis [36]. This phenotype was not observed upon treatment with the synthetic analog 5-thio, which in fact did not significantly inhibit HG-3 cell proliferation compared to natural ovo. In this case, we observed an increase in intracellular GSH com-



The finding that 5-thio inhibits human GGT and does not affect cell vitality or autophagic flux in HG-3 could provide an incentive for its potential use as an adjuvant in treating GGT-positive tumors' chemoresistance or ameliorating other pathologies characterized by high levels of GGT activity. On the other hand, the dual action of natural ovo as a reversible and non-competitive GGT inhibitor and inducer of death pathways in GGT-positive cells may point to its potential role as an anti-tumoral drug. Future experiments will be devoted to understanding whether chemical derivatives of 5-thio, used in combination with chemotherapeutic drugs, can prevent GGT-positive tumors' chemoresistance or ameliorate pathologies associated with high activity levels of GGT.

## 4. Materials and Methods

L-5-sulfanylhistidine and iso-ovothiol A were kindly provided by Jean Claude Yadan, Tetrahedron Company (Paris, France) and prepared as described in [39]. The  $^1\text{H-NMR}$  and  $^{13}\text{C-NMR}$  spectra of L-5-sulfanylhistidine derivatives are reported in the Supplementary Materials of [39]. Ovothiol A was purified from sea urchin *P. lividus* eggs, as previously described in [35]; its purity was checked via an LC-MS analysis and  $^1\text{H-NMR}$  and  $^{13}\text{C-NMR}$  data are reported in [35].

### 4.1. Enzyme Isolation and GGT Activity Assay

GGT-enriched extracts were prepared from HepG2 and HG-3 cell lines as described by Brancaccio et al. with some modifications [36]. The Hep-G2 cell line, derived from a human hepatocellular carcinoma, was generously provided by Professor M.A. Belisario of Salerno University. The HG-3 lymphoblastoid cell line was obtained by Professor A. Rosen from the Department of Clinical and Experimental Medicine, Division of Cell Biology, Linköping University, Sweden. Cells were homogenized by a potter in 4 volumes of 25 mM Tris-Cl at pH 7.5, containing 0.33 M of sucrose, 0.2 mM of EDTA, and Halt Protease and Phosphatase Inhibitor Cocktail (Merck/Sigma-Aldrich, Milan, Italy). Then re-suspended cells were centrifuged at  $9000\times g$  for 20 min and the supernatant was spun at  $24,000\times g$  for 1 h. The new pellet, resuspended in 25 mM of Tris-Cl at pH 7.35, 0.5% Triton X-100, and Phosphatase Inhibitor Cocktail, was centrifuged again at  $24,000\times g$  for 1 h. A colorimetric test was used to assay the supernatant for GGT activity. The assay buffer contained 100 mM of Tris-Cl at pH 8; each reaction contained 1 mM of GpNA as a donor substrate and 20 mM of GlyGly as an acceptor substrate. The formation of the product, p-nitroaniline, was continuously monitored at room temperature at 412 nm using a Cary 100 UV-Vis spectrophotometer (Agilent Technologies, Milan, Italy). The residual activity was reported as a percentage of GGT activity in the absence of the compounds. All substrates for GGT assay (GpNA, GlyGly) were purchased from Merck or Sigma-Aldrich (Burlington, MA, USA).

### 4.2. Derivatization and HPLC Analyses

Cell pellets ( $5 \times 10^6$  cells) were disrupted in 50  $\mu\text{L}$  of 1X PBS and centrifuged for 20 min at 13,000 rpm and 4  $^\circ\text{C}$ . Cytosolic extracts and 1 mL of culture medium were lyophilized overnight and rehydrated with 20  $\mu\text{L}$  of MQ water. Subsequently, each sample was derivatized following the protocol of Russo et al. [47]. Briefly, 100  $\mu\text{L}$  of extraction buffer (acetonitrile:  $\text{HClO}_4$  0.75 M, 1:2) was added to the rehydrated samples and vortexed for 30 s. Extracts were centrifuged for 10 min at 16,000 rpm, and 15  $\mu\text{L}$  of 2 M  $\text{K}_2\text{CO}_3$  was added to 100  $\mu\text{L}$  of cleared lysates. Insoluble cell debris and excesses of  $\text{K}_2\text{CO}_3$  were removed via another 10 min centrifugation phase at 16,000 rpm. Then, 100  $\mu\text{L}$  of supernatants was basified with 10  $\mu\text{L}$  of 50 mM  $\text{Li}_2\text{CO}_3$  and then reduced with 3  $\mu\text{L}$  of 200 mM DTT followed by a 5 min incubation phase at room temperature. Then, 25  $\mu\text{L}$  of BMC 20 mM in dimethyl sulfoxide (DMSO) was added and the samples were incubated for 30 min in the dark.

Finally, the samples were acidified with 10  $\mu$ L of 10% formic acid, vortexed for 30 s to remove CO<sub>2</sub>, and centrifuged to remove excess BMC. The samples (20  $\mu$ L) were examined via reversed-phase HPLC utilizing an Agilent Infinity 1260 apparatus (Agilent Technologies, Santa Clara, CA, USA) equipped with a Poroshell 120-C 18 column (4  $\mu$ m, 150  $\times$  4.6 mm, Agilent). Detection of thiol-BMC conjugates was accomplished by measuring absorbance at 330 nm. The column was equilibrated with a mixture of 98% solvent A (0.1% trifluoroacetic acid in water) and 2% solvent B (0.1% trifluoroacetic acid in acetonitrile) at a flow rate of 0.8 mL/min. The gradient used in [48] was modified as follows: 0.0–2 min, 2% B; 2.0 min, 3% B; 2–6 min, 3–9% B; 6–21 min, 9–45% B; 21–23 min, 45–90% B; 23–26 min, 90% B; 26–27 min, 90–2% B; 27–37, 2% B.

The thiol-BMC conjugates' identification was allowed by measuring absorbance at 330 nm. The presence of intra- and extracellular 5-thio and GSH in the samples was verified via coelution with standards of these two compounds. The quantification of both metabolites was obtained by integrating the areas of the corresponding peaks in the HPLC chromatogram, using a calibration curve built with standards of 5-thio and GSH.

#### 4.3. Cell Culture and Viability Assays

HL-60 cells (acquired from the European Collection of Cell Cultures (ECACC) and distributed in Italy by Merck-Sigma (Milan)) [49] and HG-3 cells [50] were cultured in RPMI medium supplemented with 10% FBS, 1% L-glutamine, and 1% penicillin/streptomycin (EuroClone, Milan, Italy) at 37 °C in a humidified atmosphere with 5% CO<sub>2</sub>. The concentrations of various molecules used in each experiment are specified in the corresponding figure legends. HG-3 and HL-60 cells were treated with designated concentrations of these molecules for 24 h at 37 °C in complete RPMI medium. Next, Cy-Quant dye and its background suppressor reagent (Invitrogen, Life Technologies, Milan, Italy) were added, and cells were incubated for 1 h at 37 °C in 5% CO<sub>2</sub> [51]. The fluorescence from viable cells (excitation at 485 nm/emission at 530 nm) is displayed in the graphs as a percentage of untreated (Ctrl) cells using a Synergy HT multiwell reader (Synergy HT BioTek, Milan, Italy).

#### 4.4. Intracellular ROS Measurement

Cells were incubated at a concentration of  $2 \times 10^4$  cells/mL for 30 min with a peroxide-selective probe, the chloromethyl derivative of di-chloro-fluorescein diacetate (CM-DCFDA), at a concentration of 10  $\mu$ M (Invitrogen, Life Technologies, Milan, Italy). The incubation was performed in phosphate-buffered saline (PBS) at 37 °C in a humidified 5% CO<sub>2</sub> atmosphere. Fluorescence was measured using a Synergy HT reader (BioTek, Milan, Italy) with an excitation wavelength of 485 nm and an emission wavelength of 530 nm [52].

#### 4.5. Autophagy Assay

The Cyto-ID autophagy detection kit (Enzo Life Sciences, Milan, Italy) was used to assess autophagy status following incubation with different compounds, as described in the figure legends. This kit employs a cationic amphiphilic tracer that allows precise quantification of autophagosomes within cells. The green dye, excitable at 488 nm, is formulated to minimize lysosome staining and shows bright fluorescence when incorporated into pre-autophagosomes, autophagosomes, and autolysosomes. After incubation, cells were washed and a mixture of the autophagy detection marker (Cyto-ID) and nuclear dye (Hoechst 33342) was added. Autophagosome numbers were quantified by comparing green fluorescence (Cyto-ID) to blue fluorescence (Hoechst) using a microplate fluorescence reader (Synergy HT). Microphotographs were captured with a fluorescence-inverted microscope (Axiovert Zeiss, Milan, Italy) at 400 $\times$  magnification, using either DAPI or fluorescein isothiocyanate (FITC) filters after staining [53].

#### 4.6. Statistical Analysis

Statistical analyses of data were performed via a one-way ANOVA, and differences among different treatments were evaluated using Tukey's post hoc test ( $p < 0.05$ ). The analyses were performed using the software package Prism 6 (GraphPad Software Inc., San Diego, CA, USA).

### 5. Conclusions

For the first time, we provide evidence of significant differences in the biological actions of the natural product ovo and its synthetic derivatives. Natural ovo not only acts as a potent GGT inhibitor but also as an inducer of cytotoxic autophagy in GGT-positive cells; in contrast, the chemical derivatives are less effective as GGT inhibitors and do not compromise cell viability or autophagic flux in these cells. This biological divergence appears to stem from slightly different chemical properties, which result in different mechanisms of action. Natural ovo primarily binds and inhibits external membrane-bound GGT, increasing extracellular GSH and intracellular ROS levels, thereby triggering apoptotic and autophagic pathways (see highlighted image). Conversely, 5-thio, displaying weaker GGT-inhibitory activity, interacts partially with external GGT while entering HG-3 cells, where it likely acts as an antioxidant through redox exchange with GSH. Consequently, while natural ovo shows potential as an anti-tumoral drug, the chemical derivatives may serve as adjuvants in treating GGT-positive tumors' chemoresistance or in mitigating other pathologies, characterized by high levels of GGT activity. A novel concept that emerged in this work is the dual role of natural ovo as an antioxidant or pro-oxidant, depending on the target and cellular context. In non-proliferative cells that do not overexpress GGT, natural ovo partially enters the intracellular environment [45], where it acts as an antioxidant or anti-inflammatory compound [45,54]. However, in proliferating, GGT-positive cells, its primary action as a GGT inhibitor results in pro-oxidant effects. This duality underscores the complex and context-dependent therapeutic potential of ovo and its derivatives.

**Author Contributions:** Conceptualization: I.C. and G.L.R.; supervision: I.C., M.R. and G.L.R.; data curation and formal analysis: A.Z., M.R., A.C. and I.C.; investigation: A.Z., A.C., A.M., M.R. and A.D.G.; funding acquisition: I.C.; resources: I.C., S.L. and G.L.R.; validation: S.L.; visualization: A.Z. and M.R.; writing—original draft: I.C.; writing—review and editing: I.C., S.L., M.R. and G.L.R. All authors approved the final text. All authors have read and agreed to the published version of the manuscript.

**Funding:** A.Z. has been supported by a fellowship funded by a Next-Generation EU\_PRIN 2022 Grant awarded by the Italian Ministry of University Research, no. 2022MJBEK9, CUP E53D23009970006.

**Institutional Review Board Statement:** Not applicable.

**Informed Consent Statement:** Not applicable.

**Data Availability Statement:** The datasets supporting this article will be made available on request.

**Acknowledgments:** We thank Anna Palumbo for the initial preparation of ovoidiol A and Jean Claude Yadan for providing iso-ovoidiol A and 5-thiohistidine. We acknowledge the Erasmus Mundus Joint Master's Degree "Be in Precision Medicine", University Grenoble Alpes, France, for having supported A.M.

**Conflicts of Interest:** The authors declare no competing interest.

## Abbreviations

The following abbreviations are used in this manuscript:

ANOVA	Analysis of Variance
BMC	4-Bromomethyl-7-Methoxycoumarin
CO <sub>2</sub>	Carbon Dioxide
Ctrl	Control
DAPI	4',6-Diamidino-2-Phenylindole
DMSO	Dimethyl Sulfoxide
DTT	Dithiothreitol
FBS	Fetal Bovine Serum
FITC	Fluorescein Isothiocyanate
GGT	Gamma-Glutamyl Transpeptidase
GSH	Glutathione
GSSG	Glutathione Disulfide
HPLC	High-Performance Liquid Chromatography
iso-ovoA	Iso-Ovothiol A
LC-MS	Liquid Chromatography–Mass Spectrometry
NMR	Nuclear Magnetic Resonance
ns	Not Significant
ovo	Ovothiol A
OU749	GGT Inhibitor OU749
PBS	Phosphate-Buffered Saline
RPMI	Roswell Park Memorial Institute (Medium)
ROS	Reactive Oxygen Species
TFA	Trifluoroacetic Acid
5-thio	L-5-Sulfanylhistidine

## References

1. Tate, S.S.; Meister, A.  $\gamma$ -Glutamyl Transpeptidase: Catalytic, Structural and Functional Aspects. *Mol. Cell. Biochem.* **1981**, *39*, 357–368. [\[CrossRef\]](#)
2. West, M.B.; Wickham, S.; Quinalty, L.M.; Pavlovicz, R.E.; Li, C.; Hanigan, M.H. Autocatalytic Cleavage of Human Gamma-Glutamyl Transpeptidase Is Highly Dependent on N-Glycosylation at Asparagine 95. *J. Biol. Chem.* **2011**, *286*, 28876–28888. [\[CrossRef\]](#)
3. West, M.B.; Hanigan, M.H.  $\gamma$ -Glutamyl Transpeptidase Is a Heavily N-Glycosylated Heterodimer in HepG2 Cells. *Arch. Biochem. Biophys.* **2010**, *504*, 177–181. [\[CrossRef\]](#) [\[PubMed\]](#)
4. West, M.B.; Segu, Z.M.; Feasley, C.L.; Kang, P.; Klouckova, I.; Li, C.; Novotny, M.V.; West, C.M.; Mechref, Y.; Hanigan, M.H. Analysis of Site-Specific Glycosylation of Renal and Hepatic  $\gamma$ -Glutamyl Transpeptidase from Normal Human Tissue. *J. Biol. Chem.* **2010**, *285*, 29511–29524. [\[CrossRef\]](#) [\[PubMed\]](#)
5. Bachhawat, A.K.; Yadav, S. The Glutathione Cycle: Glutathione Metabolism beyond the  $\gamma$ -Glutamyl Cycle. *IUBMB Life* **2018**, *70*, 585–592. [\[CrossRef\]](#)
6. Ballatori, N.; Krance, S.M.; Marchan, R.; Hammond, C.L. Plasma Membrane Glutathione Transporters and Their Roles in Cell Physiology and Pathophysiology. *Mol. Asp. Med.* **2009**, *30*, 13–28. [\[CrossRef\]](#) [\[PubMed\]](#)
7. Nasr, R.; Lorendeau, D.; Khonkarn, R.; Dury, L.; Pérès, B.; Boumendjel, A.; Cortay, J.-C.; Falson, P.; Chaptal, V.; Baubichon-Cortay, H. Molecular Analysis of the Massive GSH Transport Mechanism Mediated by the Human Multidrug Resistant Protein 1/ABCC1. *Sci. Rep.* **2020**, *10*, 7616. [\[CrossRef\]](#) [\[PubMed\]](#)
8. Meister, A. On the Enzymology of Amino Acid Transport. *Science* **1973**, *180*, 33–39. [\[CrossRef\]](#)
9. Zhang, H.; Forman, H.J.; Choi, J.  $\gamma$ -Glutamyl Transpeptidase in Glutathione Biosynthesis. In *Methods in Enzymology*; Sies, H., Packer, L., Eds.; Academic Press: Cambridge, MA, USA, 2005; Volume 401, pp. 468–483. [\[CrossRef\]](#)
10. Freidman, N.; Chen, I.; Wu, Q.; Briot, C.; Holst, J.; Font, J.; Vandenberg, R.; Ryan, R. Amino Acid Transporters and Exchangers from the SLC1A Family: Structure, Mechanism and Roles in Physiology and Cancer. *Neurochem. Res.* **2020**, *45*, 1268–1286. [\[CrossRef\]](#)
11. Hanigan, M.H.; Ricketts, W.A. Extracellular glutathione is a source of cysteine for cells that express gamma-glutamyl transpeptidase. *Biochemistry* **1993**, *32*, 6302–6306. [\[CrossRef\]](#)

12. Franco, R.; Cidlowski, J.A. Apoptosis and glutathione: Beyond an antioxidant. *Cell Death Differ.* **2009**, *16*, 1303–1314. [[CrossRef](#)]
13. Zhang, H.; Forman, H.J. Glutathione synthesis and its role in redox signaling. *Semin. Cell Dev. Biol.* **2012**, *23*, 722–728. [[CrossRef](#)]
14. Castellano, I.; Merlino, A.  $\gamma$ -Glutamyltranspeptidases: Sequence, structure, biochemical properties, and biotechnological applications. *Cell. Mol. Life Sci.* **2012**, *69*, 3381–3394. [[CrossRef](#)]
15. Barrios, R.; Shi, Z.-Z.; Kala, S.V.; Wiseman, A.L.; Welty, S.E.; Kala, G.; Bahler, A.A.; Ou, C.-N.; Lieberman, M.W. Oxygen-induced pulmonary injury in  $\gamma$ -glutamyl transpeptidase-deficient mice. *Lung* **2001**, *179*, 319–330. [[CrossRef](#)]
16. Lieberman, M.W.; Wiseman, A.L.; Shi, Z.Z.; Carter, B.Z.; Barrios, R.; Ou, C.N.; Chévez-Barrios, P.; Wang, Y.; Habib, G.M.; Goodman, J.C.; et al. Growth retardation and cysteine deficiency in gamma-glutamyl transpeptidase-deficient mice. *Proc. Natl. Acad. Sci. USA* **1996**, *93*, 7923–7926. [[CrossRef](#)] [[PubMed](#)]
17. Hanigan, M.H.; Pitot, H.C. Gamma-glutamyl transpeptidase—Its role in hepatocarcinogenesis. *Carcinogenesis* **1985**, *6*, 165–172. [[CrossRef](#)] [[PubMed](#)]
18. Hanigan, M.H.; Frierson, H.F.; Swanson, P.E.; De Young, B.R. Altered expression of gamma-glutamyl transpeptidase in human tumors. *Hum. Pathol.* **1999**, *30*, 300–305. [[CrossRef](#)] [[PubMed](#)]
19. Corti, A.; Franzini, M.; Paolicchi, A.; Pompella, A. Gamma-glutamyltransferase of cancer cells at the crossroads of tumor progression, drug resistance and drug targeting. *Anticancer Res.* **2010**, *30*, 1169–1181.
20. Akaydin, S.Y.; Salihoğlu, E.M.; Güngör, D.G.; Karanlık, H.; Demokan, S. Correlation between gamma-glutamyl transferase activity and glutathione levels in molecular subgroups of breast cancer. *Eur. J. Breast Health* **2020**, *16*, 72–76. [[CrossRef](#)]
21. Ruoso, P.; Hedley, D.W. Inhibition of  $\gamma$ -glutamyl transpeptidase activity decreases intracellular cysteine levels in cervical carcinoma. *Cancer Chemother. Pharmacol.* **2004**, *54*, 49–56. [[CrossRef](#)]
22. Benlloch, M.; Ortega, A.; Ferrer, P.; Segarra, R.; Obrador, E.; Asensi, M.; Carretero, J.; Estrela, J.M. Acceleration of glutathione efflux and inhibition of gamma-glutamyltranspeptidase sensitize metastatic B16 melanoma cells to endothelium-induced cytotoxicity. *J. Biol. Chem.* **2005**, *280*, 6950–6959. [[CrossRef](#)]
23. Hanigan, M.H. Gamma-glutamyl transpeptidase: Redox regulation and drug resistance. *Adv. Cancer Res.* **2014**, *122*, 103–141. [[CrossRef](#)]
24. Mitrić, A.; Castellano, I. Targeting gamma-glutamyl transpeptidase: A pleiotropic enzyme involved in glutathione metabolism and in the control of redox homeostasis. *Free Radic. Biol. Med.* **2023**, *208*, 672–683. [[CrossRef](#)]
25. Castello, G.; Mencoboni, M.; Lerza, R.; Cerruti, A.; Bogliolo, G.; Pannacciulli, I. Suppressive activity of acivicin on murine bone marrow hemopoietic progenitors. *Anticancer Res.* **1992**, *12*, 2181–2184. [[PubMed](#)]
26. Terzyan, S.S.; Cook, P.F.; Heroux, A.; Hanigan, M.H. Structure of 6-diazo-5-oxo-norleucine-bound human gamma-glutamyl transpeptidase 1, a novel mechanism of inactivation. *Protein Sci.* **2017**, *26*, 1196–1205. [[CrossRef](#)] [[PubMed](#)]
27. Yamamoto, S.; Watanabe, B.; Hiratake, J.; Tanaka, R.; Ohkita, M.; Matsumura, Y. Preventive effect of GGsTop, a novel and selective  $\gamma$ -glutamyl transpeptidase inhibitor, on ischemia/reperfusion-induced renal injury in rats. *J. Pharmacol. Exp. Ther.* **2011**, *339*, 945–951. [[CrossRef](#)] [[PubMed](#)]
28. Tuzova, M.; Jean, J.-C.; Hughey, R.P.; Brown, L.A.S.; Cruikshank, W.W.; Hiratake, J.; Joyce-Brady, M. Inhibiting lung lining fluid glutathione metabolism with GGsTop as a novel treatment for asthma. *Front. Pharmacol.* **2014**, *5*, 179. [[CrossRef](#)]
29. Takeuchi, I.; Kawamata, R.; Makino, K. Effects of GGsTop® on collagen and glutathione in the oral mucosa using a rat model of 5-fluorouracil-induced oral mucositis. *In Vivo* **2021**, *35*, 175–180. [[CrossRef](#)]
30. King, J.B.; West, M.B.; Cook, P.F.; Hanigan, M.H. A novel, species-specific class of uncompetitive inhibitors of  $\gamma$ -glutamyl transpeptidase. *J. Biol. Chem.* **2009**, *284*, 9059–9065. [[CrossRef](#)]
31. Wang, L.; Liu, Z.; He, S.; He, S.; Wang, Y. Fighting against drug-resistant tumors by the inhibition of  $\gamma$ -glutamyl transferase with supramolecular platinum prodrug nano-assemblies. *J. Mater. Chem. B* **2021**, *9*, 4587–4595. [[CrossRef](#)]
32. Castellano, I.; Seebeck, F.P. On ovothiol biosynthesis and biological roles: From life in the ocean to therapeutic potential. *Nat. Prod. Rep.* **2018**, *35*, 1241–1250. [[CrossRef](#)]
33. Osik, N.A.; Zelentsova, E.A.; Tsentlovich, Y.P. Kinetic Studies of Antioxidant Properties of Ovothiol A. *Antioxidants* **2021**, *10*, 1470. [[CrossRef](#)]
34. Murano, C.; Zuccarotto, A.; Leone, S.; Sollitto, M.; Gerdol, M.; Castellano, I.; Palumbo, A. A Survey on the Distribution of Ovothiol and ovoA Gene Expression in Different Tissues and Cells: A Comparative Analysis in Sea Urchins and Mussels. *Mar. Drugs* **2022**, *20*, 268. [[CrossRef](#)]
35. Russo, G.L.; Russo, M.; Castellano, I.; Napolitano, A.; Palumbo, A. Ovothiol Isolated from Sea Urchin Oocytes Induces Autophagy in the Hep-G2 Cell Line. *Mar. Drugs* **2014**, *12*, 4069–4085. [[CrossRef](#)] [[PubMed](#)]
36. Brancaccio, M.; Russo, M.; Masullo, M.; Palumbo, A.; Russo, G.L.; Castellano, I. Sulfur-Containing Histidine Compounds Inhibit  $\gamma$ -Glutamyl Transpeptidase Activity in Human Cancer Cells. *J. Biol. Chem.* **2019**, *294*, 14603–14614. [[CrossRef](#)] [[PubMed](#)]
37. Milito, A.; Brancaccio, M.; Lisurek, M.; Masullo, M.; Palumbo, A.; Castellano, I. Probing the Interactions of Sulfur-Containing Histidine Compounds with Human Gamma-Glutamyl Transpeptidase. *Mar. Drugs* **2019**, *17*, 650. [[CrossRef](#)]

38. Brancaccio, M.; D'Argenio, G.; Lembo, V.; Palumbo, A.; Castellano, I. Antifibrotic Effect of Marine Ovoidiol in an In Vivo Model of Liver Fibrosis. *Oxid. Med. Cell. Longev.* **2018**, *2018*, 5045734. [[CrossRef](#)] [[PubMed](#)]
39. Daunay, S.; Lebel, R.; Farescour, L.; Yadan, J.-C.; Erdelmeier, I. Short Protecting-Group-Free Synthesis of 5-Acetylsulfanyl-Histidines in Water: Novel Precursors of 5-Sulfanyl-Histidine and Its Analogues. *Org. Biomol. Chem.* **2016**, *14*, 10473–10480. [[CrossRef](#)]
40. Diederich, M.; el Yaagoubi, M.; Gérardin, P.; Wellman, M.; Siest, G. Characterization and regulatory effect of gamma-glutamyltransferase messenger RNA untranslated regions in human leukemia. *Leukemia* **1995**, *9*, 1332–1337.
41. Pompella, A.; De Tata, V.; Paolicchi, A.; Zunino, F. Expression of Gamma-Glutamyltransferase in Cancer Cells and Its Significance in Drug Resistance. *Biochem. Pharmacol.* **2006**, *71*, 231–238. [[CrossRef](#)]
42. Mena, S.; Benlloch, M.; Ortega, A.; Carretero, J.; Obrador, E.; Asensi, M.; Petschen, I.; Brown, B.D.; Estrela, J.M. Bcl-2 and Glutathione Depletion Sensitize B16 Melanoma to Combination Therapy and Eliminate Metastatic Disease. *Clin. Cancer Res.* **2007**, *13*, 2658–2666. [[CrossRef](#)]
43. Hanigan, M.H.; Gallagher, B.C.; Townsend, D.M.; Gabarra, V.  $\gamma$ -Glutamyl Transpeptidase Accelerates Tumor Growth and Increases the Resistance of Tumors to Cisplatin In Vivo. *Carcinogenesis* **1999**, *20*, 553–559. [[CrossRef](#)]
44. Hanigan, M.H.; Lykissa, E.D.; Townsend, D.M.; Ou, C.-N.; Barrios, R.; Lieberman, M.W.  $\gamma$ -Glutamyl Transpeptidase-Deficient Mice Are Resistant to the Nephrotoxic Effects of Cisplatin. *Am. J. Pathol.* **2001**, *159*, 1889–1894. [[CrossRef](#)]
45. Castellano, I.; Di Tomo, P.; Di Pietro, N.; Mandatori, D.; Pipino, C.; Formoso, G.; Napolitano, A.; Palumbo, A.; Pandolfi, A. Anti-Inflammatory Activity of Marine Ovoidiol A in an In Vitro Model of Endothelial Dysfunction Induced by Hyperglycemia. *Oxid. Med. Cell. Longev.* **2018**, *2018*, 2087373. [[CrossRef](#)]
46. Luccarini, A.; Zuccarotto, A.; Galeazzi, R.; Morresi, C.; Masullo, M.; Castellano, I.; Damiani, E. Insights on the UV-Screening Potential of Marine-Inspired Thiol Compounds. *Mar. Drugs* **2024**, *22*, 2. [[CrossRef](#)]
47. Russo, M.T.; Santin, A.; Zuccarotto, A.; Leone, S.; Palumbo, A.; Ferrante, M.I.; Castellano, I. The First Genetic Engineered System for Ovoidiol Biosynthesis in Diatoms Reveals a Mitochondrial Localization for the Sulfoxide Synthase OvoA. *Open Biol.* **2023**, *13*, 220309. [[CrossRef](#)] [[PubMed](#)]
48. Zuccarotto, A.; Sollitto, M.; Leclère, L.; Panzella, L.; Gerdol, M.; Leone, S.; Castellano, I. Molecular Evolution of Ovoidiol Biosynthesis in Animal Life Reveals Diversity of the Natural Antioxidant Ovoidiols in Cnidaria. *Free Radic. Biol. Med.* **2024**, *227*, 117–128. [[CrossRef](#)] [[PubMed](#)]
49. Gallagher, R.; Collins, S.; Trujillo, J.; McCredie, K.; Ahearn, M.; Tsai, S.; Metzgar, R.; Aulakh, G.; Ting, R.; Ruscetti, F.; et al. Characterization of the continuous, differentiating myeloid cell line (HL-60) from a patient with acute promyelocytic leukemia. *Blood* **1979**, *54*, 713–733. [[CrossRef](#)] [[PubMed](#)]
50. Rosén, A.; Bergh, A.-C.; Gogok, P.; Evaldsson, C.; Myhrinder, A.L.; Hellqvist, E.; Rasul, A.; Björkholm, M.; Jansson, M.; Mansouri, L.; et al. Lymphoblastoid Cell Line with B1 Cell Characteristics Established from a Chronic Lymphocytic Leukemia Clone by In Vitro EBV Infection. *OncoImmunology* **2012**, *1*, 18–27. [[CrossRef](#)]
51. Russo, M.; Milito, A.; Spagnuolo, C.; Carbone, V.; Rosén, A.; Minasi, P.; Lauria, F.; Russo, G.L. CK2 and PI3K Are Direct Molecular Targets of Quercetin in Chronic Lymphocytic Leukaemia. *Oncotarget* **2017**, *8*, 42571–42587. [[CrossRef](#)]
52. Russo, M.; Spagnuolo, C.; Moccia, S.; Tedesco, I.; Lauria, F.; Russo, G.L. Biochemical and Cellular Characterization of New Radio-Resistant Cell Lines Reveals a Role of Natural Flavonoids to Bypass Senescence. *Int. J. Mol. Sci.* **2021**, *23*, 301. [[CrossRef](#)] [[PubMed](#)]
53. Russo, M.; Moccia, S.; Bilotto, S.; Spagnuolo, C.; Durante, M.; Lenucci, M.S.; Mita, G.; Volpe, M.G.; Aquino, R.P.; Russo, G.L. A Carotenoid Extract from a Southern Italian Cultivar of Pumpkin Triggers Nonprotective Autophagy in Malignant Cells. *Oxid. Med. Cell. Longev.* **2017**, *2017*, 7468538. [[CrossRef](#)] [[PubMed](#)]
54. Brancaccio, M.; Milito, A.; Viegas, C.A.; Palumbo, A.; Simes, D.C.; Castellano, I. First Evidence of Dermo-Protective Activity of Marine Sulfur-Containing Histidine Compounds. *Free Radic. Biol. Med.* **2022**, *192*, 224–234. [[CrossRef](#)] [[PubMed](#)]

**Disclaimer/Publisher's Note:** The statements, opinions and data contained in all publications are solely those of the individual author(s) and contributor(s) and not of MDPI and/or the editor(s). MDPI and/or the editor(s) disclaim responsibility for any injury to people or property resulting from any ideas, methods, instructions or products referred to in the content.